

Searching for hidden sector in multiparticle production at LHC

Miguel-Angel Sanchis-Lozano^a, Edward K. Sarkisyan-Grinbaum^{b,c,*}, Salvador Moreno-Picot^d

^a*Instituto de Física Corpuscular (IFIC) and Departamento de Física Teórica,
University of Valencia-CSIC, 46100 Burjassot, Spain*

^b*Department of Physics, CERN, 1211 Geneva 23, Switzerland*

^c*Department of Physics, The University of Texas at Arlington, Arlington, TX 76019, USA*

^d*Departamento de Informática, ETSE, University of Valencia, 46100 Burjassot, Spain*

Abstract

We study the impact of a hidden sector beyond the Standard Model, *e.g.* a Hidden Valley model, on factorial moments and cumulants of multiplicity distributions in multiparticle production with a special emphasis on the prospects for LHC results.

Keywords: pp interactions at LHC, models beyond the Standard Model, multihadron correlations, Hidden Valley models, factorial and cumulant moments

Registered preprint number: arXiv:1510.08738

1. Introduction

Increasing collision energy at the LHC opens unique opportunities for searching signatures of new phenomena beyond the Standard Model (SM). On the one hand, some extensions of the SM have been suggested by looking for solutions to some pending fundamental issues in particle physics. This is the case, *e.g.*, of supersymmetry [1], and the search for supersymmetric particles is one of the fundamental goals of the LHC.

On the other hand, there are other scenarios compelled to a lesser extent by theoretical arguments, but still motivated by plausible extensions of different sectors of the SM, which should be contemplated and its phenomenology studied in detail. This is for instance the case when a new gauge group (yielding a new type of force and a new set of fundamental particles) is added to the theory, leading to new bound states with relatively low masses for some values of the model parameters. Such scenarios, generically referred as Hidden Valley models [2, 3], might have remained beyond observation so far because of an energetic barrier or weak coupling of the so-called v -particles to SM particles. Their experimental consequences have been already studied having become an objective at the LHC and other facilities, see *e.g.* [4]. For example, v -hadrons (made of v -quarks) could leave the detector undetected, leading to invisible signatures. Alternatively, for some values of the parameters of the theory, v -hadrons might decay promptly back to SM fermions thereby modifying the parton shower hadronizing to final-state particles [5].

Most signatures of New Physics in colliders are expected to be found in hard events, on the transverse plane with respect to the beams' direction (*i.e.* emitting particles with high transverse momentum p_{\perp}), where background is much reduced. In this work, however, we focus on rather diffuse soft signals in pp inelastic interactions, though expectedly tagged by hard decay products and appropriate cuts on events. For example, a non-standard state of matter from a Hidden Sector (HS) might alter particle correlations [6, 7] which can be measured to a large accuracy at the LHC. Indeed, particle correlations are known to provide a crucial information about the underlying dynamics of the multiparticle production mechanism [8, 9, 10, 11] since the beginning of high-energy (cosmic ray) physics. In particular, *genuine* correlations are especially sensitive to variations of the features of the partonic cascade leading to final-state particles.

*Corresponding author

Email addresses: Miguel.Angel.Sanchis@ific.uv.es (Miguel-Angel Sanchis-Lozano), sedward@cern.ch (Edward K. Sarkisyan-Grinbaum), Salvador.Moreno@uv.es (Salvador Moreno-Picot)

Hadron interactions at high energy are usually considered as resulting from collisions of their constituent partons, likely dominated by pairwise parton interactions. Such partonic interactions can be hard, leading to particles (or jets) with high p_{\perp} , or soft, with small transferred momentum and large multiplicities.

In order to cope with the complexity of multihadron production dynamics a multi-step scenario, most often a two-step scenario, is usually invoked. Then the resulting final state particle multiplicity distribution and its moments are given by the convolution of the distribution of particle emission sources such as strings, clusters, fireballs, clans, ladders *etc.*, and their decay and/or fragmentation distribution into partons and/or particles. Different degrees of sophistication can be achieved by introducing various phenomenological approaches to describe the observed particle multiplicity distribution.

In particular, we will rely on a phenomenological approach made in Refs. [12, 13] based on the so-called Independent Pair Parton Interaction (IPPI) model, in order to study the effects of a new physics contribution on the conventional parton cascade. Let us remark that the IPPI model does not imply no correlations among the emitted particles, but correlations stemming from the distribution probabilities describing parton interactions and their convolution, as explained later.

The study of multiplicity distributions and their properties have traditionally been a cornerstone to understand soft hadron physics. In this paper, we analyze how the multiplicity distributions of final state hadrons are modified once an extra step of an intermediate unknown state of matter is introduced in the description of the parton shower. Hereafter we will refer to this approach as the modified IPPI (mIPPI) model. Use will be made of the powerful method of the normalised factorial and cumulant moments [8, 11], allowing to extract dynamical multiparticle fluctuations and genuine correlations.

2. Inclusive correlations and factorial moments of multiplicity distributions

The study of inclusive particle correlations in multiparticle production can be performed by analyzing n -particle correlation functions and/or normalised factorial moments of multiplicity distributions [8, 9, 11]. Here we focus on the latter.

The normalized factorial moments of rank $q = 2, 3, \dots$, are defined as

$$F_q = \frac{\sum_n P(n) n(n-1) \cdots (n-q+1)}{(\sum_n P(n) n)^q}, \quad (1)$$

where $P(n)$ denotes the probability for n final-state particles (charged hadrons).

The factorial moments represent any correlation between the emitted particles in events. To extract the genuine q -particle correlations, not reducible to the product of the lower-order correlations, one uses the normalised cumulant functions, or cumulants, defined as

$$K_q = F_q - \sum_{r=1}^{q-1} \frac{(q-1)!}{r!(q-r-1)!} K_{q-r} F_r. \quad (2)$$

The factorial moments and cumulants have been extensively applied to the analysis of multihadron dynamics in different types of collisions, from e^+e^- to nucleus-nucleus interactions, in a broad range of energies [8, 9, 11].

Since F_q and $|K_q|$ grow rapidly as the rank q increases, it is convenient to consider the ratio

$$H_q = \frac{K_q}{F_q}, \quad (3)$$

which appears in a natural manner as solutions of QCD equations for the generating functions of multiplicity distributions [14].

On the other hand, normalized H_q moments are extremely sensitive to the details of multiplicity distributions (including experimental cuts on events [15]) and can be used to distinguish between different multiparticle production models and Monte Carlo generators [9, 10], and eventually the contribution of a HS as advocated in this paper.

Table 1: Probability distribution of the number of active pairs in proton-proton collisions for different TeV energies according to the IPPI model [13].

| \sqrt{s} | w_1 | w_2 | w_3 | w_4 | w_5 | w_6 | w_7 |
|------------|--------|--------|--------|--------|--------|--------|--------|
| 1.8 TeV | 0.519 | 0.269 | 0.140 | 0.072 | 0.0 | 0.0 | 0.0 |
| 7.0 TeV | 0.504 | 0.254 | 0.128 | 0.065 | 0.033 | 0.016 | 0.0 |
| 13 TeV | 0.5020 | 0.2520 | 0.1265 | 0.0635 | 0.0319 | 0.0160 | 0.0080 |

In the following, the negative binomial distribution (NBD) which is widely used in multiparticle production studies [9, 11, 16], will be employed. The distribution is given by [17]

$$P(n) = \frac{\Gamma(n+k)}{\Gamma(n+1)\Gamma(k)} \left(\frac{\langle n \rangle}{k}\right)^n \left(1 + \frac{\langle n \rangle}{k}\right)^{-n-k}, \quad (4)$$

where k^{-1} is a parameter which measures how strongly the emitted particles are correlated. One finds that

$$\frac{1}{k} = F_2 - 1. \quad (5)$$

The Poisson distribution is obtained in the limit $k \rightarrow \infty$ with $F_q = 1$ and $K_q = 0$, $\forall q$.

In pp interactions, one single NBD is found to describe satisfactorily the shape of the charged particle multiplicity distribution at up to several hundreds GeV center-of-mass (c.m.) energy. However, appearance of (shoulderlike) substructures at higher energies has been attributed to weighted superposition or convolution of more distributions stemming from more than one source or process in multiparticle production [18, 19, 20]. For reviews, see [11, 16]. This behaviour has been confirmed at LHC energies [21, 22, 23]. Thereby one can associate the growing complexity with energy of the multiplicity distribution to the increasing number of partonic interactions of the colliding particles, assuming that every interaction gives rise to a single NBD. This is in fact one of the hypotheses put forward in [12, 13] that we examine in the following section.

3. Multiparticle production as a multi-step cascade

The IPPI model [12, 13] was proposed in order reproduce the moments of multiplicity distributions in pp collisions at high energy with minimum adjustable parameters. The IPPI picture corresponds to a simplified 2-step scenario: parton binary collisions become seeds of independent cascades which hadronize (*e.g.* via string fragmentation) to the final-state multiparticle state.

Moreover, it is assumed that each pair parton interaction gives rise to a NBD, while the total distribution is ultimately described by means of the weighted sum:

$$P^{(2)}(n) = \sum_{j=1}^{j_{max}} w_j \sum_{n_i} \prod_{i=1}^j P_{\text{NBD}}(n_i, m^{(1)}, k^{(1)}) = \sum_{j=1}^{j_{max}} w_j P_{\text{NBD}}(n; jm^{(1)}, jk^{(1)}), \quad (6)$$

where w_j denotes the probability for a j -pair interaction, $m^{(1)}$ and $k^{(1)}$ correspond to the mean multiplicity and dispersion for a single pair interaction, respectively (for a sake of clarity we explicitly keep in this paper the superscript (1))¹. Note that no new adjustable parameters appear in Eq.(6) besides the distribution for j binary parton interactions which can be evaluated if some model is adopted, see *e.g.* [24, 25].

In the IPPI, the probability for j binary parton interactions per event is simply estimated as $w_j = w_1^j$, where w_1 refers to a single pair, with the normalization condition $\sum_{j=1}^{j_{max}} w_j = 1$. In Table 1 we show the values of w_j up to $w_{max} = 7$, corresponding to pp collisions at the c.m. energy \sqrt{s} of 13 TeV taken from

¹ Here and in the following, the k parameter in each step is defined as in Eq. (5), *e.g.* $1/k^{(1)} = F_2^{(1)} - 1$.

Table 2: Normalized factorial moments $F_q^{(s)}$ corresponding to the different probability distributions of Table 1. Notice that moments of rank higher than w_{max} vanish.

| \sqrt{s} | $F_1^{(s)}$ | $F_2^{(s)}$ | $F_3^{(s)}$ | $F_4^{(s)}$ | $F_5^{(s)}$ | $F_6^{(s)}$ | $F_7^{(s)}$ |
|------------|-------------|-------------|-------------|-------------|-------------|-------------|-------------|
| 1.8 TeV | 1 | 0.72 | 0.467 | 0.178 | 0.0 | 0.0 | 0.0 |
| 7.0 TeV | 1 | 0.8697 | 0.8841 | 0.8353 | 0.5979 | 0.2321 | 0.0 |
| 13 TeV | 1 | 0.914 | 1.050 | 1.231 | 1.256 | 0.940 | 0.375 |

[13] (we neglect the expectedly slight difference of w_j at c.m. energy between 13 and 14 TeV). Note that as the energy increases, more pair parton interactions would participate in each event.

Another phenomenological approach based on a QCD-inspired eikonal model can be found in [26], leading to similar results for multiplicty distributions and factorial moments as the IPPI.

Let us stress that in the current study we do not assume *ab initio* any particular type of the probability distribution. We will keep this general approach in the next section for a 3-step cascade. In fact, all the formulas developed in Appendix apply for any distribution at any stage of the multiparticle production process. Accordingly, a lot of parameters denoted as $F_q^{(p)}$ (where the superscript $p = 1, s, h$ will denote different steps of the cascade, *vide infra*) encode the complexity of the soft hadronic dynamics and hidden production mechanism. Note, however, that such parameters become fixed once the corresponding probability distributions are adopted.

3.1. Two-step cascade

One can rewrite Eq.(6) of the independent superposition of parton pair interactions in pp collisions for arbitrary particle production distributions and sources:

$$P^{(2)}(n) = \sum_{N_s} P(N_s) \sum_{n_i} \prod_{i=1}^{N_s} P^{(1)}(n_i). \quad (7)$$

Here n and N_s denote the number of (charged) particles and sources, respectively². In the notation used here, $P(N_s)$ stands now for the distribution of (fragmenting string) sources, equivalent to the parton pair interaction distribution w_j . Correspondingly, the average multiplicity can be written as $\langle n \rangle = \langle N_s \rangle m^{(1)}$ according to a 2-step description of multiparticle production.

On the other hand, the authors of [12, 13] benefit from a dramatic reduction of free parameters when assuming a weighted superposition of NBDs with shifted parameters, as can be seen in Eq.(6). In addition, since $m^{(1)}$ should be the same for any value of the rank q , only $k^{(1)}$ remains a free parameter (w_{max} was determined using a particular model). Remarkably, in the current analysis, $m^{(1)}$ cancels out in the expressions for the scaled factorial moments and cumulants.

In order to make a comparison of the results of the current study and those from [12, 13], below we assume that all $P^{(1)}(n_i)$ are NBDs. Moreover, $P(N_s)$ and w_j distributions can be formally identified. The values of $F_q^{(s)}$ up to $q = 7$ are given in Table 2 (higher rank moments vanish for $w_{max} = 7$). Let us stress that they do **not** represent a NBD.

Upon integration of the inclusive correlation functions in the central rapidity region [7], the $F_q^{(2)}$ moments can be written in terms of the moments of the subprocesses of the cascade; for example, the factorial moments of rank two read

$$F_2^{(2)} = F_2^{(s)} + \frac{F_2^{(1)}}{\langle N_s \rangle}. \quad (8)$$

Here, $F_2^{(s)} = \langle N_s(N_s - 1) \rangle / \langle N_s \rangle^2$ and $F_2^{(1)} = \langle n_1(n_1 - 1) \rangle / \langle n_1 \rangle^2$, and $\langle n_1 \rangle = m^{(1)}$ stands for the average particle multiplicity per single cascade.

²To compare with the experimental data and to get the particle multiplicity with the same charge, the multiplicity was divided by two in [12, 13]. Also note that the number of sources N_s in Eq.(7) corresponds to the number of parton pair collisions j in Eq.(6).

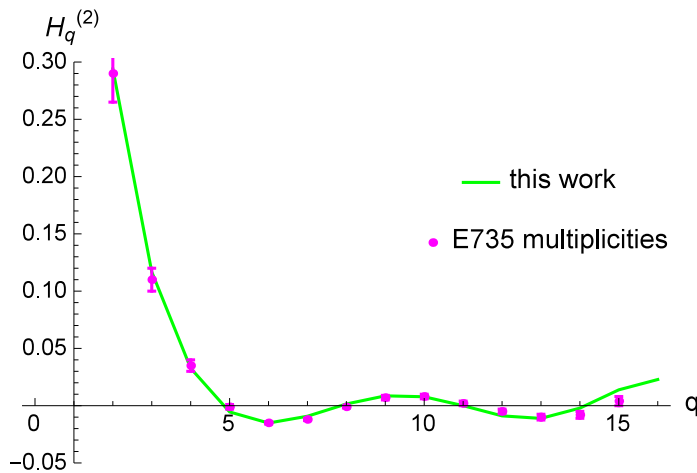


Figure 1: $H_q^{(2)}$ moments up to $q = 16$ in $p\bar{p}$ collisions at 1.8 TeV obtained in this work using expressions for a 2-step cascade and the same parameters as in [12, 13]. Very good agreement is found with the results from [12, 13] and with the calculations based on the multiplicity measurements [36]; the latter shown by circles with error bars.

The computation of higher rank $F_q^{(2)}$ moments becomes extremely involved at large q . Therefore, we have written a Prolog code (see Appendix) which provides the expressions $F_q^{(p)}$ for any value of the rank q and any number of steps p in the cascade, depending on the computer capacity available.

As shown below, we are able to reproduce (up to the percent level) the $H_q^{(2)}$ moments³ using the same values and assumptions as in Refs. [12, 13]. This accordance suggests to proceed further in the approach given here by incorporating a new step in the parton cascade following the mIPPI scheme.

Interestingly, the values of $H_q^{(2)}$ can become quite small (down to a decimal order, even approaching zero for certain values of q) while the factorial moments $F_q^{(2)}$ grow fast with q . Actually there is a delicate balance in the cancellations of Eq.(2) which can be altered when the characteristics of the parton cascade vary. Such a sensitivity could be of utility in the search for new phenomena in hadron collisions, as it is advocated here.

3.2. Three-step cascade

Let us now include an extra step in the cascade to simulate a hypothetical new stage of matter associated to a HS. The resulting multiplicity in a 3-step process should obey the following distribution:

$$P^{(3)}(n) = \sum_{N_s} P(N_s) \sum_{n_j} \prod_{j=1}^{N_s} P^{(2)}(n_j). \quad (9)$$

where $P^{(2)}$ is here defined as

$$P^{(2)}(n) = \sum_{N_h} P(N_h) \sum_{n_i} \prod_{i=1}^{N_h} P^{(1)}(n_i), \quad (10)$$

with N_h denoting the number of active hidden sources in a collision. In what follows, for the sake of simplicity we assume that $P(N_h)$ follows a Poisson distribution, *i.e.* independent production of hidden sources resulting from binary parton interactions.

In other words, the probability distribution of parton interactions remains the same as in the conventional cascade (being already adjusted to reproduce experimental data in pp collisions) while one adds another step subsequent to the initial binary parton interaction.

³As in the case of $F_q^{(p)}$ moments, here the superindex p in $H_q^{(p)}$ indicates the number of steps in the cascade: a two-step conventional cascade with $p = 2$, and the three-step cascade with $p = 3$ once a HS is included.

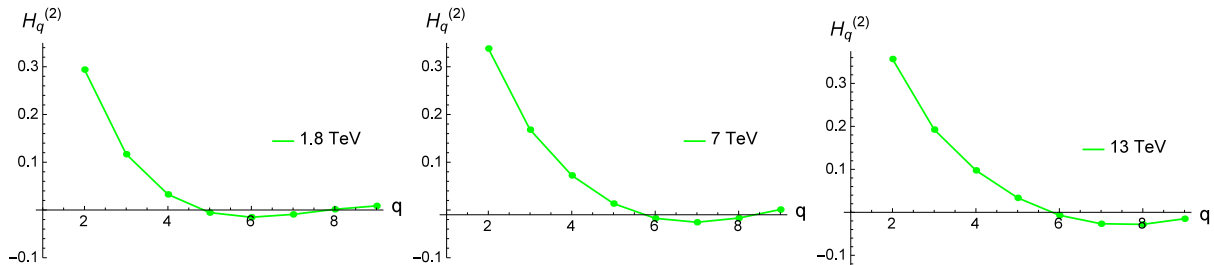


Figure 2: $H_q^{(2)}$ moments calculated up to $q = 8$ in pp collisions at $\sqrt{s} = 1.8$ TeV, 7 TeV and 13 TeV (from left to right) according to a conventional (2-step) cascade. The interpolating line is plotted to guide the eye. The crossing point (and first minimum) moves to higher q values as the collision energy increases.

Then, proceeding in the same way as in the previous section, one gets the $F_q^{(3)}$ moments in terms of the multiplicity moments from the different cascade steps. For example, the second-rank factorial moment $F_2^{(3)}$ reads

$$F_2^{(3)} = F_2^{(s)} + \frac{F_2^{(h)}}{\langle N_s \rangle} + \frac{F_2^{(1)}}{\langle N_h \rangle}, \quad (11)$$

where $\langle N_h \rangle$ and $F_2^{(h)}$ stand for the mean number and scaled moment of the hidden source distribution, respectively. In the Appendix the expressions for moments of rank up to $q = 6$ (showing increasing complexity) are provided.

As already commented, the computation of $F_q^{(p)}$ becomes especially hard for high q values and the above-mentioned Prolog code is used to obtain further factorial moments and cumulants. For example, $F_{16}^{(3)}$ contains about 100,000 terms with some coefficients of numerical order 10^9 . Needless to say again, we have checked carefully the numerical stability of the computation.

We have also checked the first $F_q^{(p)}$ moments, $p = 2$ and 3, up to $q = 8$ obtained with the Prolog code to those computed *by hand* and shown in Appendix up to $q = 6$.⁴

4. H_q -moment oscillations as a function of the rank q

QCD next-to-leading order calculations [27, 28] predict that the ratios H_q defined in Eq.(3) oscillate as a function of the rank q , crossing the q -axis and becoming negative with a minimum at

$$q_{min} \approx \frac{24}{11} \frac{1}{\gamma_0} + \frac{1}{2} + \mathcal{O}(\gamma_0), \quad (12)$$

where $\gamma_0 = (6\alpha_s/\pi)^{1/2}$ denotes the anomalous dimension at lowest order; for review, see [9, 29]. At LEP energies, it turns out that $q_{min} \approx 5$ shifting to larger values at higher energies. This prediction has been tested against experimental data and found to be observed not only in e^+e^- collisions [30, 31] but also in a variety of colliding particles and energies, including pp , pA and AA collisions [32].

It is relevant to emphasize here that in case of a single NBD, the cumulants H_q are always positive (hence no oscillations appear) and monotonically decreasing as a function of q , in clear disagreement with the QCD predictions and experimental data [9]. The study of factorial moments and cumulants also reveal difficulties that the NBD faces to describe multiparticle production in full phase space and in its small intervals [11, 33, 34, 35].

In Fig. 1 we plot the values of the $H_q^{(2)}$ moments ($q = 2$ to 16) for $\sqrt{s} = 1.8$ TeV multiplicity data, obtained through Eqs.(2) and (3) from the expressions of $F_q^{(2)}$ (a 2-step cascade). We fix the parameters

⁴In ref. [7] we already presented some of these expressions for low values of q in two-, three- and even four-step scenarios. In this paper, however, we do limit ourselves to a three-step scenario leaving the four-step scenario to be considered elsewhere. Beware also of the notation change of superscripts with respect to the present study.

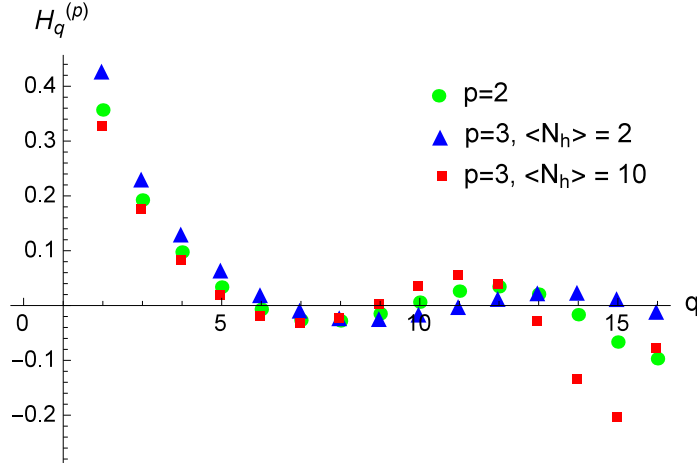


Figure 3: Predictions for $H_q^{(p)}$ moments as a function of the rank q for pp collisions at $\sqrt{s} = 13$ TeV. The circles correspond to a conventional 2-step cascade ($p = 2$) from extrapolation at lower energies using the IPPI model. The triangles and the squares correspond to a 3-step cascade ($p = 3$) using the mIPPI model (this work) with the number of hidden sources $\langle N_h \rangle = 2$ and $\langle N_h \rangle = 10$, respectively. A different pattern in the amplitude of the oscillations at high q values can be clearly observed.

for the plot alike it is done in Ref. [12], *i.e.*, assuming NBDs for all binary parton collisions with $k^{(1)} = 4.4$, and $P(N_s)$ (equivalent to the w distribution) from Table 1. The overall agreement with the results of Refs. [12, 13] and experimental data [36] is very good.

One can see the two minima in the Fig. 1. As later interpreted, this oscillatory pattern (which seems to continue for even higher ranks) is due to the fact that the probability distribution for the number of sources $P(N_s)$ (equivalently, the distribution for the number of parton pair collisions) does **not** follow a NBD. In case the distributions are all negative binomial, the resulting distribution turns out to be of the NBD type too and no oscillation pattern for $H_q^{(2)}$ shows up.

In Fig. 2 the $H_q^{(2)}$ moments obtained in the current study are shown for different pp collision c.m. energies as a function of the rank q being limited to the first minimum. Namely, the moments $H_q^{(2)}$ are plotted for $\sqrt{s} = 1.8$ TeV, 7 TeV and 13 TeV. The points were evaluated computing first the values of the $F_q^{(s)}$ moments corresponding to the source (or binary parton) probability distribution at different energies, shown in Table 2. We set $k^{(1)} = 4$ as an input in the calculations here similarly to the value of this parameter used in [12, 13]. One can see indeed that the minimum moves to the right as the pp collision energy increases, as expected.

The good agreement with the measurements shown in Fig. 1 and the expectations with the collision energy shown in a set of plots of Fig. 2 suggests the further introduction of a new step in the cascade to be interpreted as a HS, thereby studying the eventual variation of the crossing points/minima and the amplitude of the H_q oscillations.

5. HS-cascade versus a conventional cascade

5.1. Shift of the first minimum of H_q as a function of q

As explained above, the behaviour of the first minimum of H_q with the c.m. energy in pp collisions is well predicted. Let us now examine how this behaviour can be modified in a 3-step scenario under different assumptions.

In Fig. 3, the three sets of points corresponding to different scenarios at pp collisions at $\sqrt{s} = 13$ TeV are shown. The circles correspond to a conventional cascade, while the triangles and squares correspond to an extra step in the mIPPI model setting $\langle N_h \rangle = 2$ and $\langle N_h \rangle = 10$, respectively. One can see that the crossing point (and minimum) moves by about one unit to the left for $\langle N_h \rangle = 10$, and by the same amount to the right for $\langle N_h \rangle = 2$ compared to the case of a conventional cascade. Such an altered behaviour could become a hint of a HS affecting the parton evolution in multiparticle production, deserving a more detailed study.

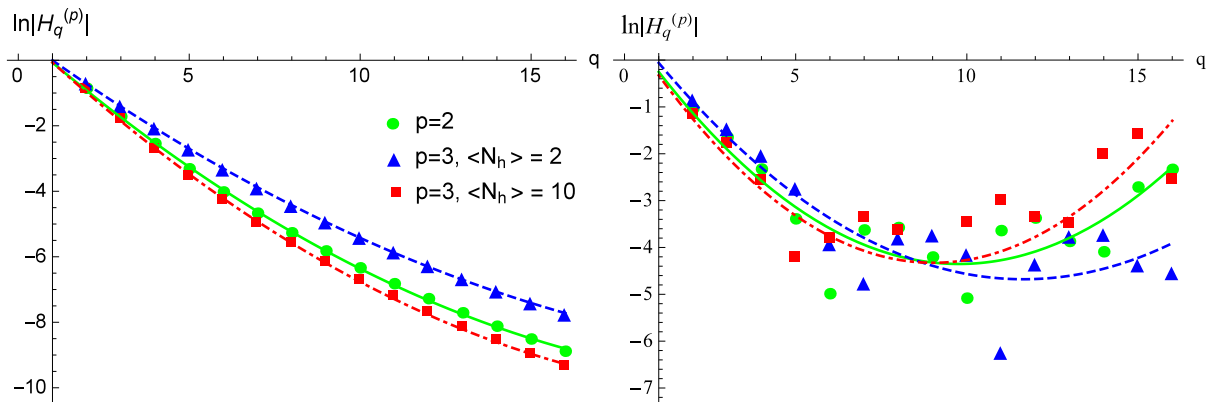


Figure 4: Values of $\ln |H_q^{(p)}|$ at $\sqrt{s} = 13$ TeV versus q for a 2-step scenario ($p = 2$, circles) and a 3-step scenario ($p = 3$) with $\langle N_h \rangle = 2$ (triangles) and $\langle N_h \rangle = 10$ (squares). Solid, dashed and dot-dashed lines correspond to parabolic fits, respectively. Left panel: superposition of NBDs with $k^{(1)} = 4$ and $k^{(s)} = k^{(h)} = 10$ as reference values. Right panel: $P(N_s)$ incorporates the values of Table 2 (not the NBD case). Notice that there are no oscillations when *all* the distributions of the convolution are of the NBD type.

5.2. Analysis of the H_q oscillation amplitude

Next let us examine the amplitude of the H_q oscillations as a function of the rank q , and its dependence on the parameters used in the mIPPI model as can be seen from in Fig. 3.

Depending on the number of hidden sources two different behaviours of the oscillation pattern of $H_q^{(3)}$ moments can be distinguished:

- For a small number of hidden sources, the oscillation amplitude becomes appreciably damped for high q values as compared to a conventional (2-step) cascade.
- For a large number of hidden sources, the oscillation amplitude is considerably larger for high q values as compared to a conventional (2-step) cascade.

These conclusions are indeed confirmed in Fig. 4 where the values of $\ln |H_q^{(p)}|$ are plotted against q for different scenarios depending on the type of the distributions used as indicated. The calculated points are shown together with the parabolic fits to them. One can see that the behaviour of the fitted curves is very different for different scenarios especially at large q values, which could thereby be relevant to detect a new physics effect according to the study presented here.

The fitted curves pass through the points in the left panel, whereas the points scatter around the curves in the right panel. This means that no oscillations appear whenever all the distributions in the superposition of Eqs.(9) and (10), including $P(N_s)$, are of the NBD type. As already commented in Section 4, this behaviour can be easily understood in the mIPPI model inasmuch the convolution of NBDs in Eq.(9) leads again to a NBD. Conversely, the oscillation pattern in the right panel emerges as a consequence of $P(N_s)$ not being a NBD.

6. Summary and final remarks

In this work we advocate that a new stage of matter, stemming from a hidden sector beyond the SM on top of the conventional partonic cascade, can be observed in multiparticle production in pp collisions at the LHC. This would result on some features of final-state particle correlations measured using the technique of factorial and cumulant moments of multiplicity distributions.

Within the modified Independent Parton Pair Interaction (mIPPI) model (with an extra step in addition to the conventional 2-step IPPI model [12, 13]), the effect of a HS on the cumulant-to-factorial moment ratio H_q of the multiplicity distributions of final-state particles strongly depends on the number of the hidden sources. A large (small) number of the sources would lead to an enhancement (softening) of the oscillation amplitude at high q values. Moreover, the crossing of the q -axis and the minimum of

the H_q -moments interpolating curve shifts to smaller (larger) q values for a large (few) number of hidden sources.

We have provided new expressions for the scaled factorial moments $F_q^{(p)}$ of the two- and three-step cascades ($p = 2$ and 3 , respectively) not given in the literature to our knowledge. Some of them (up to $q = 6$) are explicitly written in Appendix. Higher rank factorial moments can be computed by means of the Prolog code developed for this work, leading to very long and complicated formulas. We have carefully checked the correctness of our code by comparing the computed expressions to *by-hand* calculations up to $q = 8$. The numerical stability at large q was also tested by choosing, *e.g.*, a Poisson distribution for all intermediate probability distributions, and checking that the resulting values allign in the $\ln |H_q^{(p)}|$ plot as a function of q (see Fig. 4).

To conclude, we have studied the phenomenological consequences of HS physics in multiparticle production which could be useful at LHC experiments, likely requiring a low-luminosity run to reduce pile-up as much as possible. Since both –conventional and HS – processes would be present in the collected sample of events, specific cuts, such as high multiplicity, flavour tagging, high- p_\perp leptons, missing energy, *etc.*, are suggested to be applied to enrich the signatures of new physics.

Acknowledgments

This work has been partially supported by MINECO under grants FPA2011-23596 and FPA2014-54459-P, and Generalitat Valenciana under grant PROMETEOII/2014/049. One of us (M.A.S.L.) acknowledges support from IFIC under grant SEV-2014-0398 of the “Centro de Excelencia Severo Ochoa” Programme.

Appendix A. Factorial moments in 2- and 3-step scenarios

Appendix A.1. Prolog code

The structure of the problem suggests the use of declarative programming or functional programming. Finally the chosen language was Prolog [37].

The program we have used to compute the factorial moments consists of four parts [38]:

- 1) A predicate which generates all possible topologies without repetitions from a given number of final particles and a given number of disintegration steps.
- 2) A recursive predicate that counts the number of occurrences for each topology.
- 3) A predicate that groups all topologies generated under a common formula, adding all occurrences per formula.
- 4) A predicate that translates formulas generated as a latex file and as a Mathematica file.

The final result can be incorporated into a latex document, or can be incorporated directly in Mathematica to use the results in calculations and generate the corresponding graphs.

Appendix A.2. Modelled expressions for factorial moments

In this Appendix we give the expressions for the factorial moments $F_q^{(p)}$ up to $q = 6$. The superscript $p = 2$ and 3 denotes a 2- and 3-step scenario, respectively. The expressions for higher rank moments are too long to be reproduced here but can be obtained from the Prolog code developed for this work.

2-step cascade

$$F_2^{(2)} = F_2^{(s)} + \frac{F_2^{(1)}}{\langle N_s \rangle} \quad , \quad F_3^{(2)} = F_3^{(s)} + 3 \frac{F_2^{(s)} F_2^{(1)}}{\langle N_s \rangle} + \frac{F_3^{(1)}}{\langle N_s \rangle^2}$$

$$F_4^{(2)} = F_4^{(s)} + \frac{F_4^{(1)}}{\langle N_s \rangle^3} + 6 \frac{F_3^{(s)} F_2^{(1)}}{\langle N_s \rangle} + 4 \frac{F_2^{(s)} F_3^{(1)}}{\langle N_s \rangle^2} + 3 \frac{F_2^{(s)} F_2^{(1)2}}{\langle N_s \rangle^2}$$

$$F_5^{(2)} = F_5^{(s)} + \frac{F_5^{(1)}}{\langle N_s \rangle^4} + 10 \frac{F_4^{(s)} F_2^{(1)}}{\langle N_s \rangle} + 10 \frac{F_3^{(s)} F_3^{(1)}}{\langle N_s \rangle^2} + 15 \frac{F_3^{(s)} F_2^{(1)2}}{\langle N_s \rangle^2} + 5 \frac{F_2^{(s)} F_4^{(1)}}{\langle N_s \rangle^3} + 10 \frac{F_2^{(s)} F_3^{(1)} F_2^{(1)}}{\langle N_s \rangle^3}$$

$$F_6^{(2)} = F_6^{(s)} + \frac{F_6^{(1)}}{\langle N_s \rangle^5} + 15 \frac{F_5^{(s)} F_2^{(1)}}{\langle N_s \rangle} + 20 \frac{F_4^{(s)} F_3^{(1)}}{\langle N_s \rangle^2} + 15 \frac{F_3^{(s)} F_4^{(1)}}{\langle N_s \rangle^3} + 6 \frac{F_2^{(s)} F_5^{(1)}}{\langle N_s \rangle^4} +$$

$$15 \frac{F_2^{(s)} F_4^{(1)} F_2^{(1)}}{\langle N_s \rangle^4} + 10 \frac{F_2^{(s)} F_3^{(1)2}}{\langle N_s \rangle^4} + 60 \frac{F_3^{(s)} F_3^{(1)} F_2^{(1)}}{\langle N_s \rangle^3} + 45 \frac{F_4^{(s)} F_2^{(1)2}}{\langle N_s \rangle^2} + 15 \frac{F_3^{(s)} F_2^{(1)3}}{\langle N_s \rangle^3}$$

3-step cascade

$$F_2^{(3)} = F_2^{(s)} + \frac{F_2^{(h)}}{\langle N_s \rangle} + \frac{F_2^{(1)}}{\langle N_h \rangle} \quad F_3^{(3)} = F_3^{(s)} + \frac{F_3^{(h)}}{\langle N_s \rangle^2} + 3 \left[\frac{F_2^{(s)} F_2^{(h)}}{\langle N_s \rangle} + \frac{F_2^{(s)} F_2^{(1)}}{\langle N_h \rangle} + \frac{F_2^{(h)} F_2^{(1)}}{\langle N_s \rangle \langle N_h \rangle} \right] + \frac{F_3^{(1)}}{\langle N_h \rangle^2}$$

$$F_4^{(3)} = F_4^{(s)} + \frac{F_4^{(h)}}{\langle N_s \rangle^3} + \frac{F_4^{(1)}}{\langle N_h \rangle^3} + 6 \left[\frac{F_3^{(s)} F_2^{(h)}}{\langle N_s \rangle} + \frac{F_3^{(s)} F_2^{(1)}}{\langle N_h \rangle} + \frac{F_3^{(h)} F_2^{(1)}}{\langle N_s \rangle^2 \langle N_h \rangle} \right] + 4 \left[\frac{F_2^{(s)} F_3^{(h)}}{\langle N_s \rangle^2} + \frac{F_2^{(s)} F_3^{(1)}}{\langle N_h \rangle^2} + \frac{F_2^{(h)} F_3^{(1)}}{\langle N_s \rangle \langle N_h \rangle^2} \right] +$$

$$3 \left[\frac{F_2^{(s)} F_2^{(h)2}}{\langle N_s \rangle^2} + \frac{F_2^{(s)} F_2^{(1)2}}{\langle N_h \rangle^2} + \frac{F_2^{(h)} F_2^{(1)2}}{\langle N_s \rangle \langle N_h \rangle^2} \right] + 18 \frac{F_2^{(s)} F_2^{(h)} F_2^{(1)}}{\langle N_s \rangle \langle N_h \rangle}$$

$$\begin{aligned}
F_5^{(3)} = & F_5^{(s)} + \frac{F_5^{(h)}}{\langle N_s \rangle^4} + \frac{F_5^{(1)}}{\langle N_h \rangle^4} + 10 \left[\frac{F_4^{(s)} F_2^{(h)}}{\langle N_s \rangle} + \frac{F_4^{(s)} F_2^{(1)}}{\langle N_h \rangle} + \frac{F_4^{(h)} F_2^{(1)}}{\langle N_s \rangle^3 \langle N_h \rangle} \right] + \\
& 5 \left[\frac{F_2^{(s)} F_4^{(h)}}{\langle N_s \rangle^3} + \frac{F_2^{(s)} F_4^{(1)}}{\langle N_h \rangle^3} + \frac{F_2^{(h)} F_4^{(1)}}{\langle N_s \rangle \langle N_h \rangle^3} \right] + 10 \left[\frac{F_3^{(s)} F_3^{(1)}}{\langle N_h \rangle^2} + \frac{F_3^{(s)} F_3^{(h)}}{\langle N_s \rangle^2} + \frac{F_3^{(h)} F_3^{(1)}}{\langle N_s \rangle^2 \langle N_h \rangle^2} \right] + \\
& 15 \left[\frac{F_3^{(s)} F_2^{(h)2}}{\langle N_s \rangle^2} + \frac{F_3^{(s)} F_2^{(1)2}}{\langle N_h \rangle^2} + \frac{F_3^{(h)} F_2^{(1)2}}{\langle N_s \rangle^2 \langle N_h \rangle^2} \right] + 10 \left[\frac{F_2^{(h)} F_3^{(1)} F_2^{(1)}}{\langle N_s \rangle \langle N_h \rangle^3} + \frac{F_2^{(s)} F_3^{(1)} F_2^{(1)}}{\langle N_h \rangle^3} + \right. \\
& 4 \frac{F_2^{(s)} F_3^{(h)} F_2^{(1)}}{\langle N_s \rangle^2 \langle N_h \rangle} + 3 \frac{F_2^{(s)} F_2^{(h)} F_3^{(1)}}{\langle N_s \rangle \langle N_h \rangle^2} + \frac{F_2^{(s)} F_3^{(h)} F_2^{(h)}}{\langle N_s \rangle^3} + 6 \frac{F_3^{(s)} F_2^{(h)} F_2^{(1)}}{\langle N_s \rangle \langle N_h \rangle} \left. \right] + \\
& 30 \left[\frac{F_2^{(s)} F_2^{(h)2} F_2^{(1)}}{\langle N_s \rangle^2 \langle N_h \rangle} + 1.5 \frac{F_2^{(s)} F_2^{(h)} F_2^{(1)2}}{\langle N_s \rangle \langle N_h \rangle^2} \right]
\end{aligned}$$

$$\begin{aligned}
F_6^{(3)} = & F_6^{(s)} + \frac{F_6^{(h)}}{\langle N_s \rangle^5} + \frac{F_6^{(1)}}{\langle N_h \rangle^5} + \\
& 6 \left[\frac{F_2^{(s)} F_5^{(h)}}{\langle N_s \rangle^4} + \frac{F_2^{(s)} F_5^{(1)}}{\langle N_h \rangle^4} + \frac{F_2^{(h)} F_5^{(1)}}{\langle N_s \rangle \langle N_h \rangle^4} \right] + 15 \left[\frac{F_3^{(s)} F_4^{(1)}}{\langle N_h \rangle^3} + \frac{F_3^{(s)} F_4^{(h)}}{\langle N_s \rangle^3} + \frac{F_3^{(h)} F_4^{(1)}}{\langle N_s \rangle^2 \langle N_h \rangle^3} \right] + \\
& 20 \left[\frac{F_4^{(s)} F_3^{(h)}}{\langle N_s \rangle^2} + \frac{F_4^{(s)} F_3^{(1)}}{\langle N_h \rangle^2} + \frac{F_4^{(h)} F_3^{(1)}}{\langle N_s \rangle^3 \langle N_h \rangle^2} \right] + 15 \left[\frac{F_5^{(s)} F_2^{(h)}}{\langle N_s \rangle} + \frac{F_5^{(s)} F_2^{(1)}}{\langle N_h \rangle} + \frac{F_5^{(h)} F_2^{(1)}}{\langle N_s \rangle^4 \langle N_h \rangle} \right] + \\
& 15 \left[5 \frac{F_2^{(s)} F_4^{(h)} F_2^{(1)}}{\langle N_s \rangle^3 \langle N_h \rangle} + \frac{F_2^{(s)} F_4^{(h)} F_2^{(h)}}{\langle N_s \rangle^4} + 3 \frac{F_2^{(s)} F_2^{(h)} F_4^{(1)}}{\langle N_s \rangle \langle N_h \rangle^3} + \frac{F_2^{(s)} F_4^{(1)} F_2^{(1)}}{\langle N_h \rangle^4} + \frac{F_2^{(h)} F_4^{(1)} F_2^{(1)}}{\langle N_s \rangle \langle N_h \rangle^4} \right] + \\
& 10 \left[\frac{F_2^{(s)} F_3^{(h)2}}{\langle N_s \rangle^4} + 8 \frac{F_2^{(s)} F_3^{(h)} F_3^{(1)}}{\langle N_s \rangle^2 \langle N_h \rangle^2} + \frac{F_2^{(s)} F_3^{(1)2}}{\langle N_h \rangle^4} + \frac{F_2^{(h)} F_3^{(1)2}}{\langle N_s \rangle \langle N_h \rangle^4} \right] + \\
& 60 \left[\frac{F_3^{(s)} F_3^{(h)} F_2^{(h)}}{\langle N_s \rangle^3} + 2 \frac{F_3^{(s)} F_2^{(h)} F_3^{(1)}}{\langle N_s \rangle \langle N_h \rangle^2} + \frac{F_3^{(s)} F_3^{(1)} F_2^{(1)}}{\langle N_h \rangle^3} + 2.5 \frac{F_3^{(s)} F_3^{(h)} F_2^{(1)}}{\langle N_s \rangle^2 \langle N_h \rangle} + \frac{F_3^{(h)} F_3^{(1)} F_2^{(1)}}{\langle N_s \rangle^2 \langle N_h \rangle^3} \right] + \\
& 45 \left[\frac{F_4^{(s)} F_2^{(1)2}}{\langle N_h \rangle^2} + \frac{F_4^{(s)} F_2^{(h)2}}{\langle N_s \rangle^2} + \frac{150 F_4^{(s)} F_2^{(h)} F_2^{(1)}}{45 \langle N_s \rangle \langle N_h \rangle} + \frac{F_4^{(h)} F_2^{(1)2}}{\langle N_s \rangle^3 \langle N_h \rangle^2} \right] + \\
& 15 \left[\frac{F_3^{(s)} F_2^{(h)3}}{\langle N_s \rangle^3} + \frac{F_3^{(s)} F_2^{(1)3}}{\langle N_h \rangle^3} + \frac{F_3^{(h)} F_2^{(1)3}}{\langle N_s \rangle^2 \langle N_h \rangle^3} + 18 \frac{F_3^{(s)} F_2^{(h)} F_2^{(1)2}}{\langle N_s \rangle \langle N_h \rangle^2} + 15 \frac{F_3^{(s)} F_2^{(h)2} F_2^{(1)}}{\langle N_s \rangle^2 \langle N_h \rangle} \right] + \\
& 180 \left[\frac{F_2^{(s)} F_3^{(h)} F_2^{(1)2}}{\langle N_s \rangle^2 \langle N_h \rangle^2} + \frac{F_2^{(s)} F_2^{(h)} F_2^{(1)} F_3^{(1)}}{\langle N_s \rangle \langle N_h \rangle^3} \right] + \\
& 60 \frac{F_2^{(s)} F_2^{(h)2} F_3^{(1)}}{\langle N_s \rangle^2 \langle N_h \rangle^2} + 135 \frac{F_2^{(s)} F_2^{(h)2} F_2^{(1)2}}{\langle N_s \rangle^2 \langle N_h \rangle^2} + 45 \frac{F_2^{(s)} F_2^{(h)} F_2^{(1)3}}{\langle N_s \rangle \langle N_h \rangle^3}
\end{aligned}$$

References

- [1] H. E. Haber and G. L. Kane, Phys. Rept. **117** (1985) 75.
- [2] M. J. Strassler and K. M. Zurek, Phys. Lett. B **651**, 374 (2007) [hep-ph/0604261].
- [3] J. Kang and M. A. Luty, JHEP **0911** (2009) 065 [arXiv:0805.4642] [hep-ph]].
- [4] S. Alekhin *et al.*, arXiv:1504.04855 [hep-ph].
- [5] M. J. Strassler, arXiv:0806.2385 [hep-ph].
- [6] M.-A. Sanchis-Lozano, Int. J. Mod. Phys. A **24** (2009) 4529 [arXiv:0812.2397 [hep-ph]].
- [7] M.-A. Sanchis-Lozano and E. Sarkisyan-Grinbaum, arXiv:1409.5262 [hep-ph].
- [8] E. A. De Wolf, I. M. Dremin and W. Kittel, Phys. Rept. **270** (1996) 1 [hep-ph/9508325].
- [9] I. M. Dremin and J. W. Gary, Phys. Rept. **349**, 301 (2001) [hep-ph/0004215].
- [10] J. Manjavidze and A. Sissakian, Phys. Rept. **346**, 1 (2001) [hep-ph/0105245].
- [11] For a comprehensive review on wide aspects of multiparticle production emphasising correlation studies, see: W. Kittel, E. A. De Wolf, *Soft Multihadron Dynamics* (World Scientific, Singapore, 2005).
- [12] I. M. Dremin and V. A. Nechitailo, Phys. Rev. D **70** (2004) 034005 [hep-ph/0402286].
- [13] I. M. Dremin and V. A. Nechitailo, Phys. Rev. D **84** (2011) 034026 [arXiv:1106.4959 [hep-ph]].
- [14] I. M. Dremin, Phys. Lett. B **313** (1993) 209.
- [15] R. Ugoccioni, A. Giovannini and S. Lupia, Phys. Lett. B **342** (1995) 387 [hep-ph/9410340].
- [16] J. F. Grosse-Oetringhaus and K. Reygers, J. Phys. G **37**, 083001 (2010) [arXiv:0912.0023 [hep-ex]].
- [17] A. Giovannini and L. Van Hove, Z. Phys. C **30** (1986) 391.
- [18] G. N. Fowler, E. M. Friedlander, R. M. Weiner and G. Wilk, Phys. Rev. Lett. **56** (1986) 14.
- [19] A. Giovannini and R. Ugoccioni, Phys. Rev. D **59** (1999) 094020 [Phys. Rev. D **69** (2004) 059903] [hep-ph/9810446].
- [20] A. Giovannini and R. Ugoccioni, Phys. Rev. D **68** (2003) 034009 [hep-ph/0304128].
- [21] I. Zborovský, J. Phys. G **40** (2013) 055005 [arXiv:1303.7388 [hep-ph]].
- [22] P. Ghosh and S. Muhuri, Phys. Rev. D **87** (2013) 094020 [arXiv:1402.6820 [hep-ph]].
- [23] J. Adam *et al.* [ALICE Collaboration], arXiv:1509.07541 [nucl-ex].
- [24] A. B. Kaidalov and K. A. Ter-Martirosyan, Phys. Lett. B **117** (1982) 247.
- [25] S. G. Matinyan and W. D. Walker, Phys. Rev. D **59** (1999) 034022 [hep-ph/9801219].
- [26] P. C. Beggio and E. G. S. Luna, Nucl. Phys. A **929** (2014) 230 [arXiv:1308.6192 [hep-ph]].
- [27] I. M. Dremin, Phys. Lett. B **341** (1994) 95, [Phys. Lett. B **348** (1995) 711 (E)] [hep-ph/9408300].
- [28] M. A. Buican, C. Forster and W. Ochs, Eur. Phys. J. C **31** (2003) 57 [hep-ph/0307234].
- [29] V. A. Khoze and W. Ochs, Int. J. Mod. Phys. A **12** (1997) 2949 [hep-ph/9701421].
- [30] K. Abe *et al.* [SLD Collaboration], Phys. Lett. B **371**, 149 (1996) [hep-ex/9601010].
- [31] P. Achard *et al.* [L3 Collaboration], Phys. Lett. B **577**, 109 (2014) [hep-ex/0110072].

- [32] I. M. Dremin, V. A. Nechitailo, M. Biyajima and N. Suzuki, Phys. Lett. B **403**, 149 (1997) [hep-ph/9704318].
- [33] E. K. G. Sarkisyan, Phys. Lett. B **477**, 1 (2000) [hep-ph/0001262].
- [34] G. Abbiendi *et al.* [OPAL Collaboration], Eur. Phys. J. C **11**, 239 (1999) [hep-ex/9902021].
- [35] G. Abbiendi *et al.* [OPAL Collaboration], Phys. Lett. B **523**, 35 (2001) [hep-ex/0110051].
- [36] E735 Collaboration, F. Turkot et al., Nucl. Phys A **525** (1991) 165
- [37] W.F. Clocksin and C.S. Mellish, *Programming in Prolog*, 5th edition. 2003. Springer-Verlag. ISBN 3-540-00678-8
- [38] M.-A. Sanchis-Lozano, E. K. Sarkisyan-Grinbaum, S. Moreno-Picot, paper in preparation